MCB
Journals.ASM.org

The AMPK β2 Subunit Is Required for Energy Homeostasis during Metabolic Stress

Biplab Dasgupta,[a] Jeong Sun Ju,[b] Yo Sasaki,[e] Xiaona Liu,[a] Su-Ryun Jung,[c] Kazuhiko Higashida,[c] Diana Lindquist,[d] and Jeffrey Milbrandt[e]

Department of Pediatrics, Division of Hematology and Oncology,[a] and Imaging Research Center, Department of Radiology,[d] Cincinnati Children's Hospital Medical Center, Cincinnati, Ohio, USA, and Departments of Neurology[b] and Internal Medicine[c] and Department of Genetics and HOPE Center for Neurological Disorders,[e] Washington University School of Medicine, St. Louis, Missouri, USA

AMP activated protein kinase (AMPK) plays a key role in the regulatory network responsible for maintaining systemic energy homeostasis during exercise or nutrient deprivation. To understand the function of the regulatory β2 subunit of AMPK in systemic energy metabolism, we characterized β2 subunit-deficient mice. Using these mutant mice, we demonstrated that the β2 subunit plays an important role in regulating glucose, glycogen, and lipid metabolism during metabolic stress. The β2 mutant animals failed to maintain euglycemia and muscle ATP levels during fasting. In addition, β2-deficient animals showed classic symptoms of metabolic syndrome, including hyperglycemia, glucose intolerance, and insulin resistance when maintained on a high-fat diet (HFD), and were unable to maintain muscle ATP levels during exercise. Cell surface-associated glucose transporter levels were reduced in skeletal muscle from β2 mutant animals on an HFD. In addition, they displayed poor exercise performance and impaired muscle glycogen metabolism. These mutant mice had decreased activation of AMPK and deficits in PGC1α-mediated transcription in skeletal muscle. Our results highlight specific roles of AMPK complexes containing the β2 subunit and suggest the potential utility of AMPK isoform-specific pharmacological modulators for treatment of metabolic, cardiac, and neurological disorders.

AMP activated protein kinase (AMPK) plays a crucial role in maintaining systemic energy homeostasis through its coordinated actions on the central nervous system and peripheral tissues (54). Loss of AMPK function causes metabolic abnormalities in mice and defects in development and growth, cell polarity, and structure in plants, *Drosophila*, and rodents (1, 10, 33). Moreover, AMPK is necessary for caloric restriction-mediated longevity in *Caenorhabditis elegans* (19). AMPK is an intracellular energy sensor. When intracellular levels of ATP decrease, a corresponding increase in AMP leads to activation of AMPK, a step that is vital for restoring intracellular energy balance via AMPK-dependent inhibition of energy-consuming biosynthetic processes and concomitant activation of pathways that increase ATP production.

AMPK is a multisubstrate, heterotrimeric serine/threonine kinase consisting of one α, one β, and one γ subunit. The mammalian genome encodes two α, two β, and three γ subunits. The N terminus of the α subunit contains the catalytic domain as well as a phosphorylation site for upstream kinases that regulate its activity (9). The γ subunits are nucleotide binding regulatory subunits that bind AMP. The conserved C terminus of the β subunit interacts with both the α and γ subunits and plays an obligatory role in AMPK complex formation (10, 46). In addition, β subunits contain a conserved carbohydrate-binding domain that allows AMPK to function as a glycogen sensor (37, 42).

While AMPK is present in all tissues, the individual AMPK subunits display considerable variation in tissue-specific expression, subunit association, and subcellular localization. Earlier studies demonstrated that the α2 catalytic subunit associates exclusively with β1 in slow-twitch (type I) soleus muscle fibers, whereas in fast-twitch (type II) extensor digitorum longus (EDL) muscle fibers, α2 associates with both β1 and β2 subunits (7, 49). Furthermore, in skeletal muscle, the α2, but not the α1, subunit translocates to the nucleus in response to exercise (38). The β1 subunit is highly expressed in brain and liver, whereas β2 is most highly expressed in skeletal muscle (48). In addition, β1 is predominantly located in the nucleus in neurons (50) and neural stem cells, whereas β2 is predominantly cytoplasmic (10). The subcellular localization of β subunits is undoubtedly important for AMPK function, as studies in yeasts showed that they direct localization of the catalytic α subunit and thus regulate substrate selection (45).

To study the functions of the β2 subunit, we generated and characterized β2-deficient mice. Here, we report that the β2-deficient mice are overtly normal but display severe deficiencies in energy homeostasis when subjected to metabolic stress. These studies illustrate an important role for the β2 subunit in regulating AMPK function during times of increased energy demands.

MATERIALS AND METHODS

Generation of AMPK β2-deficient mice. Embryonic stem (ES) cells (clone AL0483; *129/Ola*) containing an AMPKβ2 gene trap allele were obtained from Bay Genomics, San Francisco, CA. Briefly, AMPKβ2 gene trap ES cells were microinjected into blastocysts derived from superovulated pregnant mice, and these blastocysts were injected into pseudopregnant C57BL/6 females. Chimeric males (129/Ola mixed background) were mated with C57BL/6 females, and germ line transmission was confirmed by PCR genotyping of tail DNA. All procedures were carried out in

Received 23 June 2011 Returned for modification 15 August 2011
Accepted 7 May 2012
Published ahead of print 14 May 2012
Address correspondence to Biplab Dasgupta, biplab.dasgupta@cchmc.org, or Jeffrey Milbrandt, jmilbrandt@wustl.edu.

doi:10.1128/MCB.05853-11

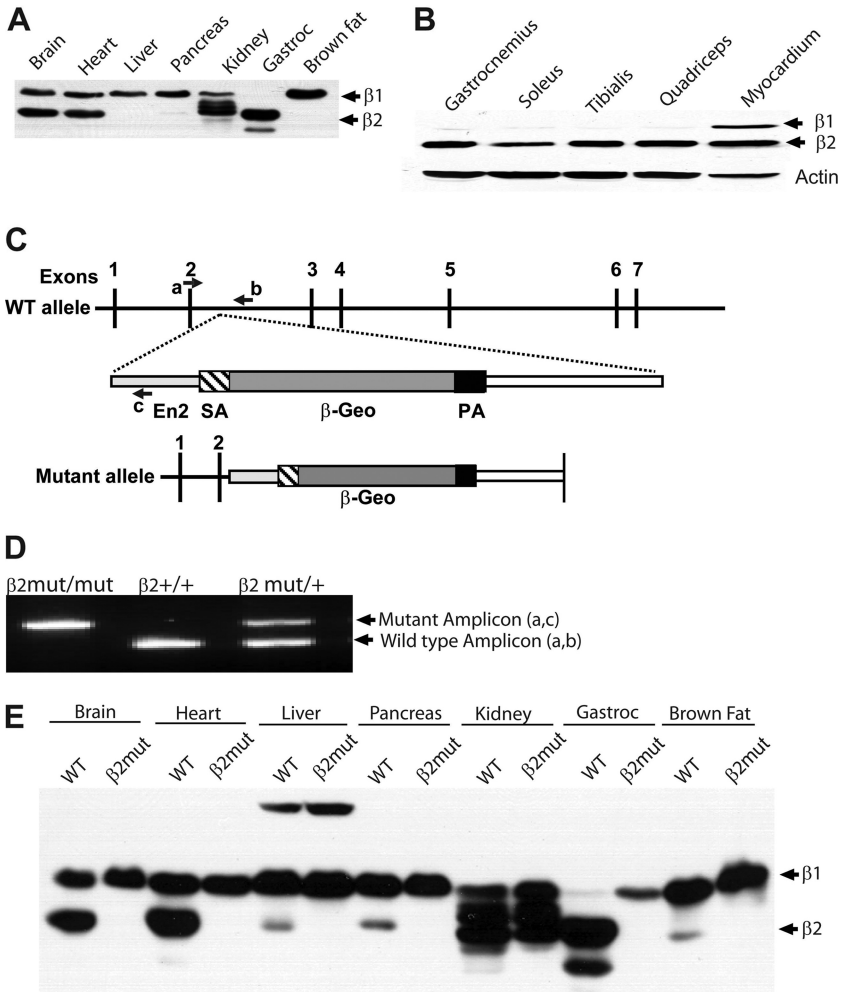

FIG 1 Skeletal muscle predominantly expresses the AMPK β2 subunit. (A) Immunoblot analysis using β1/β2 C-terminus-specific antibody detects expression of β1 and β2 in WT tissues. (B) Immunoblot analysis of type I (soleus and quadriceps), type II (tibialis), and mixed (gastrocnemius) skeletal muscle and cardiac muscle using β1/β2 C-terminus-specific antibody. (C) Numbers 1 to 7 are exons of the β2 gene; a, b, and c are genotyping primers for wild-type and mutant β2 alleles. SA, splice acceptor; β-Geo, β-galactosidase-neomycin resistance cassette; PA, polyadenylation signal. (D) Genotyping PCR of tail DNA from β2 mutant (−/−), WT (+/+), and heterozygote (+/−) animals. (E) Immunoblot analysis using β1/β2 C-terminus-specific antibody showing the absence of β2 subunit expression in all organs of β2 mutant mice.

the Washington University animal care facility. The insertion site of the gene trap within the β2 locus was identified using a PCR ladder approach. Ten forward primers were designed 250 bp apart within exon 2 and the following intron, where the β-geo trap was putatively inserted. The reverse primer was designed from the En2 sequence located in the gene trap N terminus (primer c in Fig. 1C). PCR fragments were obtained and sequenced to identify the site of insertion. Primer a, which was closest to the insertion site, was used for subsequent PCR genotyping reactions (Fig. 1C). The wild-type (WT) β2 fragment was detected using primer a and a reverse primer (primer b in Fig. 1C) corresponding to β2 intronic sequences located ~300 nucleotides (nt) downstream of the gene trap 5′ junction. Animals were backcrossed for at least 10 generations with C57BL/6 mice to achieve a pure C57BL/6 background.

Immunoprecipitation, subcellular fractionation, and Western blot analysis. Freshly dissected tissues were lysed with MAPK lysis buffer (20 mM Tris-HCl [pH 7.5], 150 mM NaCl, 1 mM EGTA, 1 mM EDTA, 1% Triton X-100, 2.5 mM sodium pyrophosphate, 1 mM β-glycerophosphate, 1 mM sodium vanadate, 1 mM phenylmethylsulfonyl fluoride [PMSF], 1 mM dithiothreitol [DTT], and protease inhibitor cocktail). Membranes were prepared from skeletal muscle by following an established protocol (44). AMPK was immunoprecipitated with AMPKα1/2 antibody (Cell Signaling Technology, Beverly, MA). The primary antibody was incubated with 100 μg of protein lysate at 4°C for 16 h, followed by incubation with 10 μl of protein G beads for 1 h at 4°C. The immune complexes were then collected by centrifugation. The immunoprecipitated proteins were electrophoresed through an SDS-polyacrylamide gel and analyzed by standard immunoblot analysis. Immunoblot analysis was carried out with the following primary antibodies: AMPKβ1/β2 C terminus, AMPKα1/2, phospho-AMPKα1/2^{Thr172}, ACC, phospho-ACC^{Ser79}, phosphorylated RaptorSer^{792} (pRaptorSer^{792}), pULK1^{Ser555}, pS6Ser$^{235/236}$, p4EBP1^{Thr70}, actin, and tubulin (all from Cell Signaling Technology), pFOXO3 Ser^{413}, pFOXO3^{Ser588} (kind gift from Anne Brunet, Stanford University), and Glut4 (rabbit polyclonal, a kind gift from Paul Hruz, Washington University, St. Louis, MO). Detection was performed using anti-rabbit or anti-mouse horseradish peroxidase (HRP)-linked secondary antibodies (Cell Signaling Technology), followed by chemiluminescence (Millipore, Billerica, MA). Densitometric scans were performed using Gel-Pro-Analyzer software.

SAMS peptide assay. SAMS peptide assays to monitor AMPK activity were performed as described previously, with some modifications (13, 53). Briefly, tissues were homogenized with a motorized tissue homoge-

nizer for 20 to 30 s in 500 μl of ice-cold buffer (225 mM mannitol, 75 mM sucrose, 10 mM Tris-HCl [pH 7.4], 1 mM EDTA, 5 mM sodium pyrophosphate, 50 mM NaF, 1 mM dithiothreitol, 1.5 mM PMSF, and protease inhibitor cocktail). The homogenate was centrifuged for 1 min at 15,000 × *g*, and the supernatant was stored in aliquots at −80°C for later determination of protein concentration and AMPK activity. AMPK holoenzyme was immunoprecipitated using AMPKα1/2 antibody and protein G-agarose from 200 μg of protein lysate; the beads were washed twice with kinase buffer (20 mM Tris-HCl [pH 7.5], 7.5 mM $MgCl_2$, 0.5 mM EGTA, 25 mM β-glycerophosphate, 0.5 mM sodium vanadate, 1 mM PMSF, and protease inhibitor cocktail) and used in the kinase reaction (25 μl of immunoprecipitated beads). The kinase reaction mixture containing immunoprecipitated AMPK, 100 μM SAMS peptide substrate, 200 μM AMP, and 1 μl (2 μCi) of [^{32}P]ATP was incubated at 30°C for 20 min with gentle agitation. The reaction was centrifuged to pellet the beads, and 20 μl of supernatant was spotted on Whatman P81 paper. The filter papers were washed thrice with 1% phosphoric acid and once with acetone and air dried, and radioactivity was counted using a scintillation counter.

Measurement of glucose, insulin, serum cholesterol, lipids, and glycogen. Glucose levels were determined using an Accu-Chek II glucometer (Roche Diagnostics) with blood collected from the tail vein. Insulin levels were determined by an enzyme-linked immunosorbent assay (ELISA) kit (Singulex insulin assay) with mouse insulin standards (ALPCO) at the Immunoassay Core of the Core Laboratory for Clinical Studies at Washington University School of Medicine. Total triglycerides and total cholesterol were measured using Infinity cholesterol and triglyceride kits (Fisher Scientific), and free fatty acids were determined by a two-step method using reagents from WAKO Chemicals according to the manufacturer's instructions. These measurements were done in the Clinical Nutrition Research Unit (CNRU) at Washington University School of Medicine. Muscle samples were stored at −80°C until analyzed. Muscle glycogen was analyzed with a glycogen assay kit (BioVision) according to the manufacturer's instructions. Briefly, ~25 mg of muscle was ground in 0.3 M perchloric acid at 4°C. Muscle glycogen content was measured by a colorimetric assay using an ELX-800 universal plate reader (Bio-Tek, Winooski, VT) set at an absorbance reading of 570 nm.

Glucose tolerance and insulin sensitivity test. For glucose tolerance tests (GTT), mice were injected with dextrose (2 g/kg body weight) and blood glucose levels were measured at 0, 30, 60, and 120 min after injection. Plasma was also collected at 0, 15, and 30 min after glucose injection and submitted to the Washington University RIA Core Facility for insulin measurements. For insulin tolerance tests (ITT), mice were fasted for 4 h; human insulin (0.75 U/kg body weight; 100 U/ml; Lilly) was injected intraperitoneally and blood glucose levels were measured at 0, 30, 60, and 120 min after insulin injection. All animal procedures were approved by the Washington University Animal Studies Committee.

Glucose uptake by skeletal muscle. Uptake of 2-deoxy-D-[1,2-^{3}H] glucose (2.25 μCi) by isolated epitrochlearis and extensor digitorum longus muscle was performed as previously described (22). Briefly, after dissection, muscles were allowed to recover for 60 min in flasks containing 2 ml of Krebs-Henseleit bicarbonate buffer (KHB) with 8 mM glucose, 32 mM mannitol, and a gas phase of 95% O_2-5% CO_2. The flasks were placed in a shaking incubator maintained at 35°C. After recovery, some muscles were incubated in the same medium containing 2 mM 5-aminoimidazole-4-carboxyamide ribonucleoside (AICAR; Toronto Research Chemicals) or 0.3 μM insulin (100 U/ml; Lilly) for 60 min. After treatment, the muscles were rinsed for 10 min at 29°C in 2 ml of oxygenated KHB containing 40 mM mannitol to remove glucose and treatment agents. After the rinse step, muscles were incubated for 10 min at 29°C in flasks containing 2 ml of KHB with 1 mM 2-[1,2-^{3}H]deoxyglucose (2-DG; 1.5 μCi/ml) and 36 mM [^{14}C]mannitol (0.2 μCi/ml), with a gas phase of 95% O_2-5% CO_2, in a shaking incubator. The muscles were then blotted, clamp-frozen, and processed for determination of intracellular [^{3}H]2-DG-6-phosphate accumulation and extracellular space.

Measurement of muscle ATP. ATP and AMP were analyzed by high-performance liquid chromatography (HPLC) as described previously, with minor modifications (11). Briefly, muscle tissue was snap-frozen in liquid nitrogen to preserve metabolites. Nucleotides were extracted from frozen muscle tissue by sonication in 1 M $HClO_4$ (1 ml/100 mg tissue). Homogenates were placed on ice for 5 min and centrifuged at 5,000 × *g* for 10 min. After centrifugation, the supernatant was neutralized with ice-cold 3 M K_2CO_3, diluted 1:50 in 10 mM phosphate buffer (pH 7.0), and analyzed by HPLC with an LC-18T reverse-phase column (Supelco, Bellefonte, PA) at a flow rate of 1 ml/min. The absorbance at 254 nm was recorded, and the amount of ATP or AMP was quantified from the chromatogram by interpolation from a curve obtained using AMP and ATP standards (Sigma).

Treadmill test. For analysis of exercise-induced gene expression in skeletal muscle, 4- to 6-week-old control and β2-deficient animals were allowed to run for 25 min on a treadmill at 15 m/min. All animals were returned to their cages after the run. Mice were sacrificed 2 or 6 h after the run, and skeletal muscles were isolated, flash-frozen in liquid nitrogen, and stored at −80°C. For the stress test, 2- to 6-month-old WT and β2 knockout (KO) animals were allowed to run on a treadmill at 10 m/min (time zero). The speed was increased 3 m/min every 3 min. The time was recorded when they came in contact with the stimulus shock for 7 s (exhaustion), at which time the animals were removed from the treadmill.

Magnetic resonance imaging (MRI). Mice were anesthetized with 5% isoflurane in air and maintained on 1.5% isoflurane in air for the duration of the experiment. Animals were scanned on a Bruker 7T Biospec system using a Bruker 72-mm-quadrature coil. Axial and coronal images were acquired using a spin echo sequence with TR/TE of 400/10.2 ms and 19 slices of 1.25-mm and 1-mm thicknesses, respectively, with in-plane resolutions of 0.25 mm by 0.25 mm.

Images were imported into ImageJ (Rasband) and manually segmented three times. The area of each fat segment was measured for each slice of each mouse and converted to volume using the resolution and slice thickness. The final estimate was the average of the three individual estimates.

Quantitative RT-PCR analysis. RNA was isolated from skeletal muscle using TRIzol (Invitrogen, San Diego, CA). Quantitative reverse transcriptase PCR (RT-PCR) analysis was performed using Sybr green methodology on a model 7500 Fast instrument (Applied Biosystems, Foster City, CA).

Primer sequences. Primer sequences were as follows: PGC1α (forward), AATCAGACCTGACACAACGC; PGC1α (reverse), GCATTCCT CAATTTCACCAA; cytochrome *c* (forward), GGAGGCAAGCATAAGA CTGG; cytochrome *c* (reverse), TCCATCAGGGTATCCTCTCC; Cox 4 (forward), AGAAGGAAATGGCTGCAGAA; Cox 4 (reverse), GCTCGG CTTCCAGTATTGAG; CPT1b (forward), TTGCCCTACAGCTGGCTC ATTTCC; and CPT1b (reverse), GCACCCAGATGATTGGGATACTGT.

Statistical methods. Student's *t* test was used to calculate statistical significance, with a P of <0.05 representing a statistically significant difference.

RESULTS

The AMPK β subunits are differentially expressed in tissues. To examine AMPK β subunit expression patterns, we performed immunoblot analysis on tissue lysates from adult wild-type (WT) mice using an antibody directed against the highly conserved C termini of the β subunit. This antibody recognizes β1 and β2 subunits, which can be distinguished by their electrophoretic mobilities. These studies showed that β1 and β2 are coexpressed at relatively equivalent levels in adult brain and heart. However, in skeletal muscle, β2 was, in essence, the only β subunit present. In adult liver, pancreas, kidney, and brown fat, β1 was the predominant β subunit expressed (Fig. 1A and B). In the kidney, multiple β1 isoforms were detected (Fig. 1A and E).

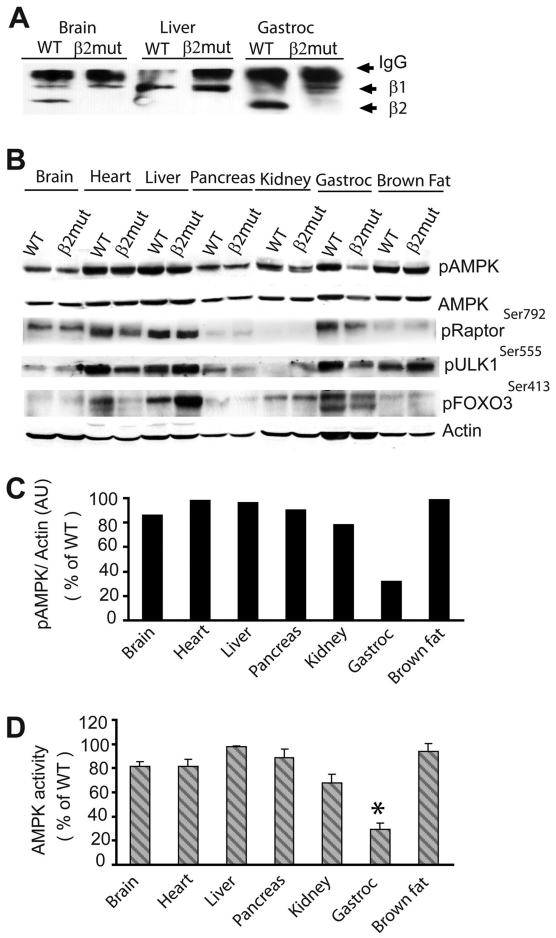

FIG 2 Loss of AMPK β2 causes extensive loss of AMPK activity in skeletal muscle. (A) Immunoblot using the β1/β2 antibody following immunoprecipitation of α subunits with α1/2 antibody. AMPK α/β1 and/or AMPK α/β2 complexes were detected in brain, liver, and gastrocnemius muscle. (B) Immunoblot analysis of phosphorylated AMPK (pAMPK), pRaptor, pULK1, and pFOXO3 in organs of β2 mutant mice using phospho-specific antibodies. β-Actin was used as a loading control. (C) Densitometric analysis of pAMPK in organs of β2 mutant mice. AU, arbitrary units. (D) AMPK activity analysis from tissue lysates of WT and β2 mutant animals using SAMS peptide as a substrate. *, $P < 0.001$.

To identify specific functions of the β2 subunit, we generated β2-deficient mice. The β2 gene was disrupted using gene trap technology in ES cells (Bay Genomics), and these ES cells were used to generate animals harboring the mutant β2 allele. In these mutant mice, the β2 gene was interrupted after exon 2 by the insertion of a β-Geo cassette (Fig. 1C and D). The β2 mutant animals grew normally with no overt abnormalities, were fertile, and lived to old age. Immunoblot analysis confirmed the loss of β2 protein in all tissues of these mutant animals (Fig. 1E).

To examine whether the β1 protein in β2-deficient muscle is complexed with an AMPK α subunit, we immunoprecipitated the α1 and α2 subunits and performed immunoblotting using β1/2 C-terminus-specific antibody (Fig. 2A). While AMPK α subunits were found predominantly in complexes with β2 in WT gastrocnemius muscle, α/β1-containing complexes are clearly present in β2-deficient muscle. While both β1- and β2-containing AMPK complexes were detected in brain, the liver contained almost exclusively β1-associated complexes, in accord with the extremely low expression of β2 in this organ.

To monitor the effect of β2 subunit loss on AMPK activity, we examined AMPK α subunit phosphorylation in tissues from β2 mutant animals using immunoblot analysis. We found that AMPK α subunit phosphorylation was largely similar in all tissues except skeletal muscle (32.2% of WT), which predominantly expresses β2 (Fig. 2B and C). pAMPK levels were also slightly lower in β2 mutant kidney. A direct examination of AMPK function using a SAMS peptide assay also showed decreased activity, consistent with the immunoblot results with the pAMPK antibody (Fig. 2D).

We further examined the phosphorylation state of selected AMPK downstream substrates in tissues from β2 mutant mice. AMPK negatively regulates mTOR by phosphorylating Raptor to inhibit protein translation and ribosome biogenesis (21, 25). The modulation of mTOR activity by AMPK is reflected in the altered phosphorylation of the mTOR substrates S6 and 4EBP1. It also phosphorylates the mammalian autophagy protein Ulk1 to protect cells during nutrient stress (14, 31). In addition, AMPK phosphorylation of FOXO3 regulates oxidative stress resistance (20). Although phosphorylation of AMPK sites of Raptor (Ser^{792}), Ulk1(^{Ser555}), and FOXO3 (Ser^{413}) was clearly reduced in AMPKβ2-deficient skeletal and cardiac muscle, total expression levels of these proteins were comparable between WT and β2-deficient animals (data not shown). This indicates that AMPK-dependent phosphorylation of these substrates is dependent on AMPKβ2 complexes (Fig. 2B). The liver primarily expresses the β1 subunit, and accordingly, there were no differences in Raptor or ULK1 phosphorylation between WT and β2 mutant animals (Fig. 2B). We observed an unexpectedly high level of FOXO3 phosphorylation in liver from β2 mutant animals. Collectively, these results demonstrate organ-specific regulation of AMPK substrate phosphorylation by AMPKβ2 complexes and show that β2 mutant skeletal muscle is deficient in AMPK activity despite the compensatory increase in β1 levels.

AICAR-stimulated glucose uptake is impaired in skeletal muscle of β2-deficient mice. AMPK regulates glucose metabolism in part by increasing glucose utilization in muscle and inhibiting gluconeogenesis in the liver. To assess the impact of β2 subunit loss on glucose metabolism, we measured serum glucose levels in β2-deficient animals. The plasma glucose level in β2-mutant animals trended higher but did not reach statistical significance (Fig. 3A). Next, to evaluate the acute response of these mutant animals to a glucose challenge, we injected dextrose (2 g/kg). However, no evidence of glucose intolerance was observed, despite the 70% decrease in muscle AMPK activity (Fig. 3B).

Pharmacological activation of AMPK stimulates glucose uptake in skeletal muscle via the glucose transporter Glut4 in skeletal muscle. We utilized isolated muscle preparations to examine AMPK-mediated increases in glucose uptake in response to the AMPK activator AICAR. Muscles from WT and β2 mutant mice were incubated in the presence or absence of AICAR (2 mM) for 60 min, and glucose uptake was measured by monitoring intracellular [^{3}H]2-DG content (13). We found that Glut4 expression and basal glucose uptake were similar in WT and β2-deficient muscles (Fig. 3C and D); however, in contrast to WT muscle, there was no AICAR-mediated increase in glucose uptake in muscles from β2 mutant animals (Fig. 3D and E).

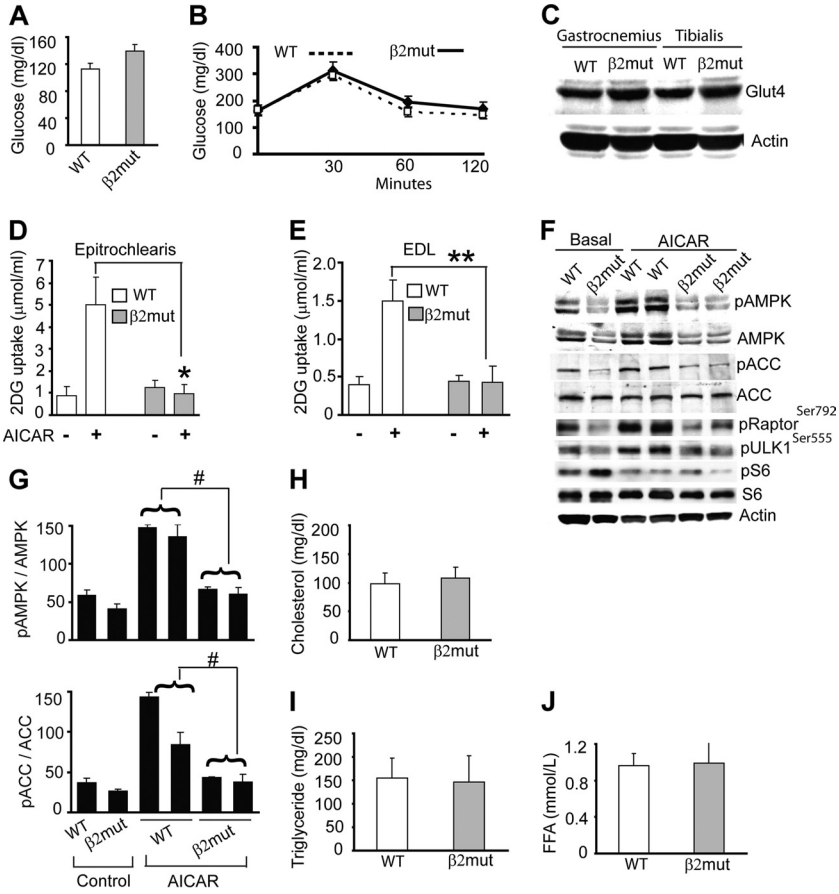

FIG 3 AMPK β2 mutant animals have normal glucose and lipid profiles but impaired AICAR-stimulated glucose uptake. Shown are basal glucose levels (A) and glucose tolerance tests (B) in WT and β2 mutant mice ($n = 6$ to 10 for each group). (C) Immunoblot analysis of total Glut4 in WT and β2 mutant skeletal muscle. (D and E) AICAR-stimulated 2-[^{3}H]deoxyglucose uptake by epitrochlearis and extensor digitorum longus (EDL) muscles isolated from WT and β2 mutant animals ($n = 6$ to 10 for each group). *, $P = 0.0001$; **, $P = 0.003$. (F) Immunoblot using pAMPK, pACC, pRaptor, pULK, and pS6 antibodies shows AICAR-stimulated levels of active AMPK and phosphorylation of AMPK downstream targets in gastrocnemius muscle of WT and β2 mutant animals. Total AMPK, ACC, and S6 are also shown. β-Actin was used as a loading control. (G) Densitometry of pAMPK and pACC levels in control and AICAR-stimulated WT and β2 mutant gastrocnemius muscle. #, $P \leq 0.005$. (H to J) Levels of serum cholesterol, triglyceride, and free fatty acid (FFA) in β2 mutant animals ($n = 6$ to 10 for each group).

Intraperitoneal injection of AICAR (1 mg/g body weight) failed to significantly increase pAMPK and pACC levels in β2-deficient gastrocnemius muscle (Fig. 3F and G). We also examined the role of AMPKβ2 complex in AICAR-stimulated phosphorylation of selected AMPK substrates in skeletal muscle from these animals. As shown in Fig. 3F, phosphorylation of Raptor and Ulk1 was decreased both basally and after AICAR treatment in β2-deficient gastrocnemius muscle, although total protein levels were unaffected (data not shown). Phosphorylation of the mTOR target S6 was higher basally but was reduced similarly by AICAR treatment in WT and β2 mutant muscles. These results indicate that AMPKβ2 complexes participate in the AICAR-stimulated phosphorylation of these canonical AMPK targets in skeletal muscle.

Active AMPK regulates lipid metabolism in part by inhibiting cholesterol and fatty acid synthesis in the liver. In β2-deficient mice, these metabolites were present at normal levels, perhaps reflecting the relatively normal level of liver AMPK (Fig. 3H to J). Overall, these results showed that while glucose uptake and metabolism, as well as cholesterol and lipid metabolism, were similar in WT and β2 mutant animals under basal conditions, maximal glucose uptake in response to AICAR-stimulated AMPK activation was impaired in β2-deficient skeletal muscle.

The AMPK β2 subunit is required for metabolic homeostasis in response to nutritional stress. In addition to controlling basal metabolism, AMPK plays a crucial role in maintaining energy homeostasis during periods of metabolic stress. Although no overt abnormalities were observed in β2-deficient animals under normal conditions, we suspected that their response to stressful conditions might be abnormal. To pursue this idea, we first examined their response to nutritional deprivation. Two-month-old WT and β2 mutant animals were fasted for 24 or 48 h. All WT and mutant animals survived this challenge; however, while monitoring the animals, we noticed that mutant animals moved more sluggishly than WT mice after 48 h of fasting. We measured serum glucose and lipid levels in these animals and found that even after 48 h of fasting, serum cholesterol, free fatty acid, and triglyceride levels in WT and mutant animals were similar (Fig. 4A to C). In contrast, plasma glucose levels in fasted mutant animals were much lower than those in fasted WT mice (Fig. 4D). Insulin levels

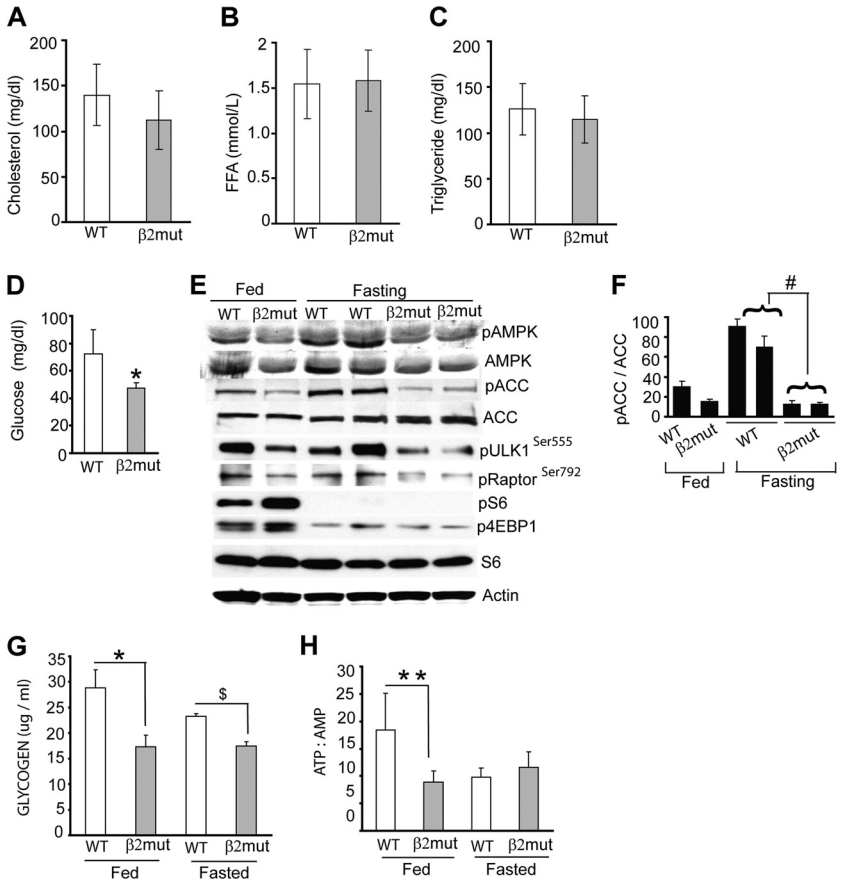

FIG 4 Reduced basal muscle glycogen and fasting hypoglycemia in AMPK β2-deficient mice. Histograms show serum cholesterol (A), free fatty acid (FFA) (B), and triglyceride (C) levels in WT and β2 mutant animals ($n = 8$ per group). (D) Glucose levels in 48-h-fasted WT and β2 mutant animals ($n = 7$ for each group). *, $P = 0.002$. (E) Immunoblot showing levels of pAMPK, pACC, pRaptor, pULK1, p4EBP1, and pS6 as well as total AMPK, ACC, and S6 in gastrocnemius muscle from WT and β2-deficient mice after fasting. β-Actin was used as a loading control. (F) Densitometry of pACC levels in fed and fasted WT and β2 mutant gastrocnemius muscle. #, $P = 0.005$. (G) Glycogen content in skeletal muscle from fed and fasted (48 h) WT and β2 mutant animals. *, $P = 0.01$; $, $P = 0.004$. (H) ATP/AMP ratio in skeletal muscle of fed and 48-h-fasted WT and β2 mutant animals. **, $P = 0.05$.

also appeared lower in mutant mice, but these reductions did not reach statistical significance (data not shown). Immunoblot analysis with pAMPK-specific antibodies was performed to examine AMPK activation in response to food restriction. While fasting induced higher levels of pAMPK and pACC in WT mice, no changes in phosphorylated AMPK or ACC were observed in skeletal muscle from fasted β2-deficient mice (Fig. 4E and F). We next examined the phosphorylation of selected AMPK substrates in skeletal muscle of fed and fasted animals. In fed β2 mutant animals, levels of pRaptor (Fig. 4E) but not total raptor (data not shown) were reduced. The phosphorylation of the mTOR targets S6 and 4EBP1 was increased in fed mutant animals but was downregulated by fasting in a fashion similar to that observed in WT fasted animals (Fig. 4E).

We next measured muscle glycogen content in fed and fasted β2 mutant animals, as muscle glycogen is a prime source of glucose and energy during prolonged fasting. The basal glycogen content of these mutant mice in the fed state was significantly lower than that of control animals (Fig. 4G). Furthermore, while fasting caused ~20% reduction in muscle glycogen in WT animals, β2-deficient mice completely failed to break down muscle glycogen even after a 48-h fast (Fig. 4G).

We also assessed basal energy content in β2-deficient gastrocnemius muscle by measuring the ATP/AMP ratio. In WT animals, the ATP/AMP ratio decreased considerably after fasting for 48 h; however, this ratio was unchanged in fasted β2 mutant mice (Fig. 4H). Collectively, these studies suggest that decreased AMPK activation in β2-deficient skeletal muscle results in aberrant glucose homeostasis, decreased muscle glycogen, and reduced muscle energy stores.

β2-deficient mice demonstrate metabolic syndrome upon exposure to a high-fat diet. Animals fed a high-fat (Western) diet (HFD) develop metabolic syndrome, a condition characterized by hyperglycemia, insulin resistance, and hyperlipidemia. The role of AMPK in regulating fatty acid metabolism encouraged us to examine whether β2 mutant animals developed any of these metabolic abnormalities when maintained on an HFD. Wild-type animals weighed ~30% more after 12 weeks on an HFD than animals fed normal chow; in contrast, β2-deficient animals on an HFD weighed 48% more than their chow-fed counterparts (Fig. 5A). The differences appeared to be more noticeable in males, but this difference was not significant. We also measured body fat content (30) and found that β2 mutant mice maintained on an HFD had a significantly larger amount of fat (4 to 5 times) than

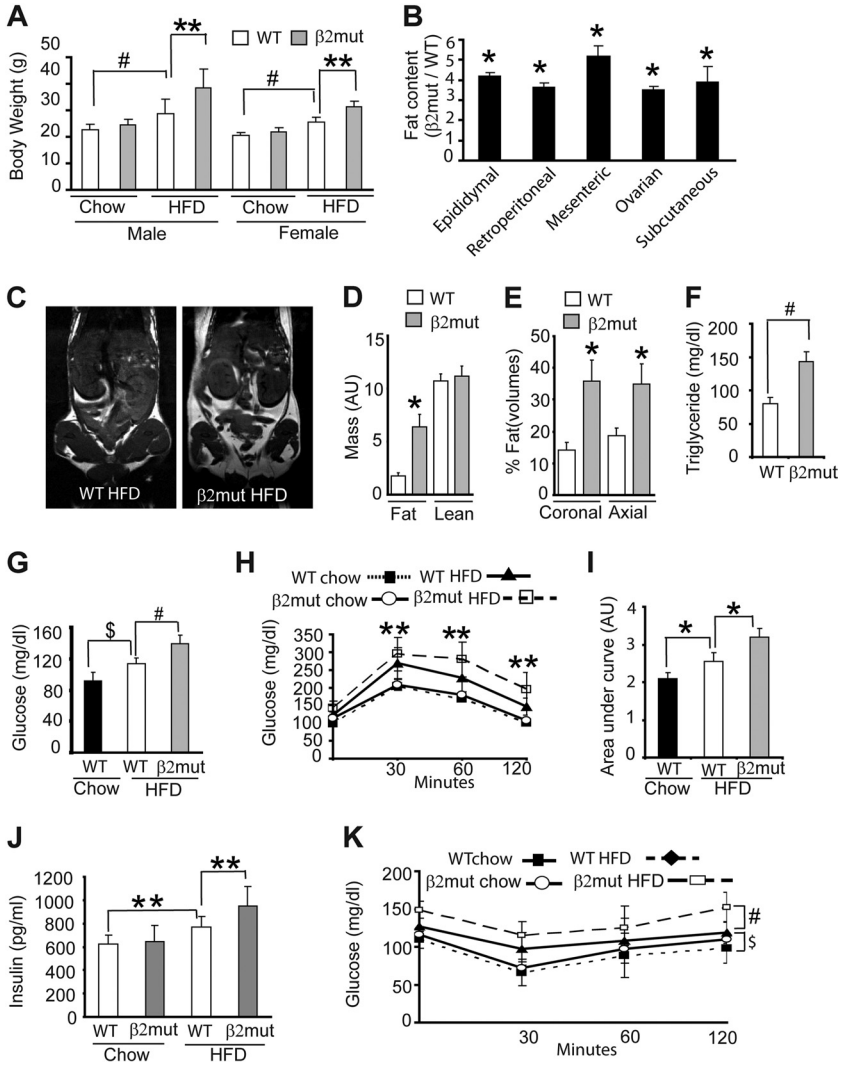

FIG 5 AMPK β2 mutant mice maintained on an HFD develop metabolic syndrome. (A) Body weights of WT and β2 mutant animals after 12 weeks on normal chow or an HFD ($n = 8$ for each group). **, $P = 0.02$; #, $P = 0.0003$. (B) Fat content (expressed as ratio of β2 mutant to WT) of animals maintained on an HFD for 12 weeks ($n = 8$ for each group). *, $P < 0.001$. (C) Representative MRI images (coronal section) of WT and β2 mutant mice on an HFD. The areas of high signal intensity are fatty areas. (D and E) Quantitation of fat and lean mass (D) and fat volumes (E) of WT and β2 mutant mice on an HFD. AU, arbitrary units. (F) Serum triglyceride levels of WT and β2 mutant animals after 12 weeks on an HFD ($n = 8$ for each group). #, $P = 0.0003$. (G to I) Basal glucose levels (G) and glucose tolerance tests (H and I) of WT and β2 mutant animals maintained on the indicated diet ($n = 8$ for each group). $, $P = 0.001$; #, $P = 0.009$; **, $P = 0.04$; *, $P \leq 0.03$. (J and K) Steady-state insulin levels (J) and insulin sensitivity test (K) in WT and β2 mutant animals fed normal chow or an HFD ($n = 7$ for each group). **, $P = 0.05$; #, $P = 0.006$; $, $P = 0.05$.

comparably fed WT animals (Fig. 5B). Magnetic resonance imaging of WT and β2 mutant animals on HFD revealed a significant increase in fat mass versus lean mass (Fig. 5C and D) and an increase in fat volume (Fig. 5E) in β2 mutant animals compared to WT animals.

The metabolic syndrome induced by HFD is characterized by increases in serum triglyceride levels. Serum cholesterol and free fatty acid levels in β2-deficient and wild-type animals maintained on an HFD were comparable (data not shown). In contrast, we found that triglyceride levels in β2-deficient animals on an HFD were nearly double those found in their WT counterparts (Fig. 5F). We also examined serum glucose levels, and as expected, WT mice fed an HFD developed hyperglycemia. This HFD-induced increase in serum glucose was further enhanced in β2 mutant animals (Fig. 5G). Consistent with these results, glucose tolerance tests revealed HFD-induced changes that were more severe in β2-deficient mice (Fig. 5H and I). While basal insulin levels were normal in β2-deficient mice, these animals manifested an exaggerated increase in insulin levels when maintained on an HFD (Fig. 5J). To investigate whether insulin resistance caused by an HFD was exacerbated in β2 mutant animals, we performed insulin sensitivity tests on WT and mutant animals maintained on a normal diet or HFD. All animals maintained on an HFD showed classical signs of insulin resistance; however, these changes were clearly more severe in β2 mutant animals (Fig. 5K). These results indicate that loss of the AMPK β2 subunit disrupts metabolic homeostasis and results in features associated with metabolic syndrome.

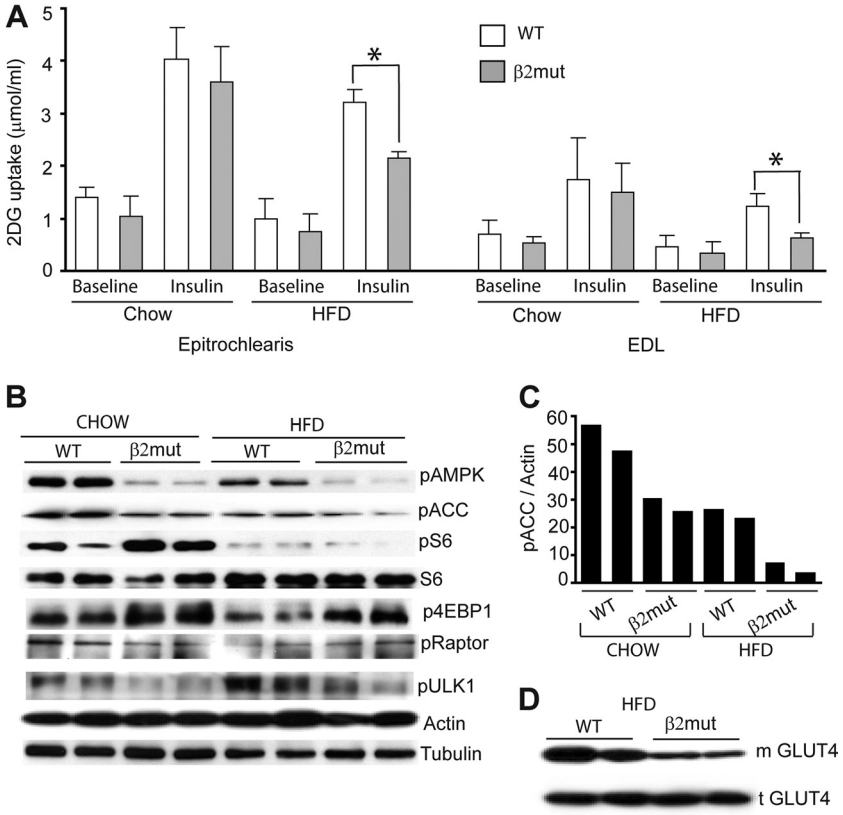

FIG 6 Reduced insulin-stimulated glucose uptake and plasma membrane-associated glucose transporter expression in β2 mutant animals. (A) Baseline and insulin-stimulated 2-DG uptake in isolated skeletal muscles from WT and β2 mutant animals fed normal chow or an HFD. *, $P < 0.05$. (B) Immunoblot analysis of epitrochlearis muscle from above animals using antibodies to pAMPK, pACC, pRaptor, pULK1, p4EBP1, pS6, and total S6. β-Actin and tubulin were used as loading controls. (C) Densitometry of pAMPK and pACC levels in epitrochlearis muscle of chow- or HFD-fed WT and β2 mutant mice. (D) Immunoblot analysis of epitrochlearis muscle from same animals using Glut4 antibodies to show total (t) and membrane-associated (m) Glut4.

AMPK plays a crucial role in skeletal muscle glucose uptake, and animals on an HFD show impaired glucose transport (17). We sought to determine whether insulin-stimulated glucose uptake is compromised in β2 mutant animals fed either a normal diet or an HFD. We measured insulin-stimulated glucose uptake *ex vivo* using epitrochlearis and EDL muscles isolated from WT or β2 mutant animals maintained on a normal diet or an HFD. We found that baseline glucose ([^{3}H]-2-DG) uptake in muscles from mutant animals was lower than that observed in their WT counterparts, although it did not reach statistical significance (Fig. 6A). Glucose uptake was stimulated by insulin in both WT and mutant mice fed normal chow, but this response was less robust in β2-deficient animals (Fig. 6A). Insulin-stimulated glucose uptake was compromised in all mice fed an HFD, with more severe deficits observed in β2-deficient animals (Fig. 6A). In concert with these results, AMPK activity is severely reduced in muscles of β2 mutant mice fed an HFD (~92% compared to WT chow-fed animals) (Fig. 6B). ACC phosphorylation was concomitantly reduced in muscle from β2 mutant animals on an HFD versus normal chow (Fig. 6B and C). We also investigated whether the AMPKβ2 complex is essential for downstream phosphorylation of selected substrates in response to fasting (Fig. 6B). We found little diet-dependent alteration in Raptor phosphorylation and no significant differences in WT versus β2 mutant animals. We did observe significant increases in the levels of pS6 and p4EBP1 in chow-fed β2 mutant animals. The phosphorylation of these proteins was dramatically reduced in both WT and mutant animals maintained on an HFD, suggesting additional AMPK-independent regulation of their function during metabolic stress.

Since AMPK plays an important role in the translocation of glucose transporters from the intracellular space to the plasma membrane, we reasoned that reduced AMPK activity in muscles of the mutant animals might lead to reduced insulin-stimulated translocation of Glut4, the major glucose transporter in skeletal muscle (27). We prepared total protein lysates and plasma membrane fractions from epitrochlearis muscles of WT and β2-deficient mice maintained on an HFD. Immunoblot analysis showed that total Glut4 levels were not significantly altered in β2 mutant mice fed a normal diet (Fig. 6D, lower panel); however, membrane-associated Glut4 levels were markedly reduced in mutant animals on an HFD (Fig. 6D, upper panel). Taken together, our results demonstrate that animals lacking the AMPK β2 subunit become hypoglycemic during acute metabolic stress (fasting) and develop features reminiscent of metabolic syndrome when maintained on an HFD.

The β2 subunit is required for normal exercise performance. AMPK is a major regulator of skeletal muscle energy metabolism. It is activated in response to the increased energetic load produced by exercise. The increased AMPK activity allows the muscle to adapt to both short-term (by stimulating glucose utilization) and long-term (by augmenting breakdown of glycogen and fatty acids)

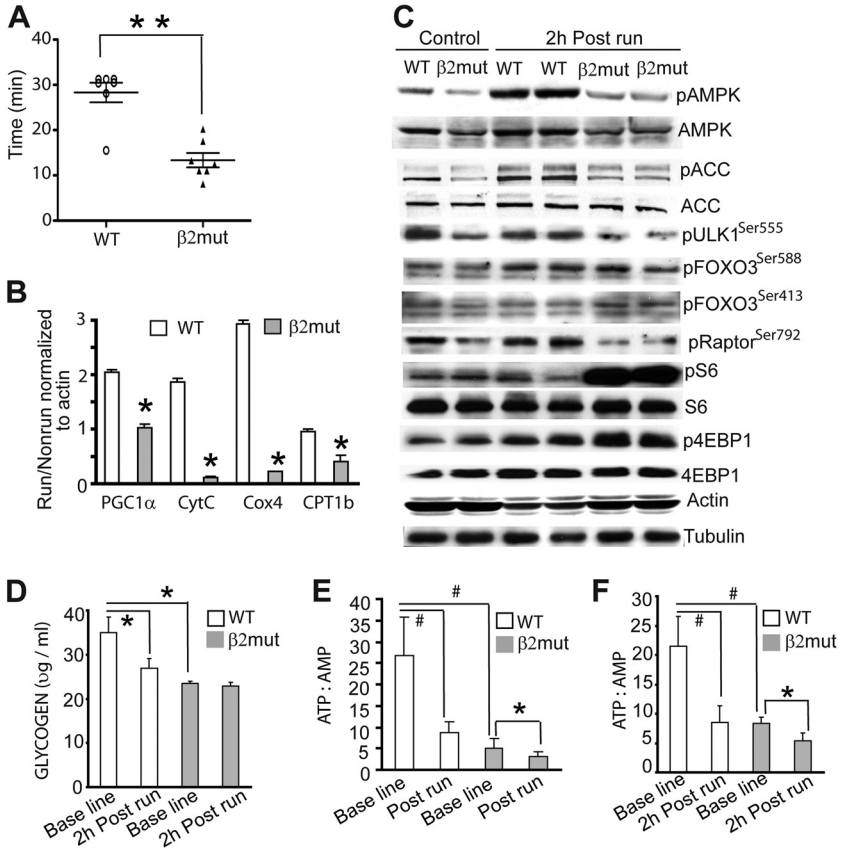

FIG 7 Poor exercise endurance in β2 mutant animals. (A) Performance of WT and β2 mutant animals in the treadmill running assay ($n = 7$ for each group). **, $P < 0.0001$. (B) Quantitative RT-PCR analysis of gastrocnemius muscle from WT and β2 mutant mice 6 h after and before the treadmill run. For each group, data were normalized to β-actin expression. *, $P < 0.05$. (C) Immunoblot analysis of pAMPK, pACC, pRaptor, pULK1, pFOXO3, p4EBP1, pS6, total S6, and total 4EBP1 in gastrocnemius muscle from WT and β2 mutant mice showing basal and exercise-induced levels of AMPK activation. Note that total AMPK but not total ACC levels were reduced in β2 mutant animals. β-Actin and tubulin were used as loading controls. (D to F) Glycogen content at baseline and 2 h postrun (D) and ATP/AMP ratio at baseline and immediately after run (E) and 2 h postrun (F) in the epitrochlearis muscle of WT and β2 mutant animals. *, $P < 0.03$; #, $P < 0.01$.

energy demands of the muscle. To test whether a lack of β2 subunit in muscle affected exercise performance, we initially tested motor coordination and neuromuscular function in β2 mutant mice. We evaluated these animals using rotarod and sensorimotor tests and measured nerve conduction velocities, but no abnormalities were observed (data not shown). We next monitored the endurance of age-matched WT and β2 mutant animals using a treadmill test. We found that regardless of age (i.e., 2 to 6 months), β2-deficient mice became exhausted after a much shorter time than their WT counterparts (Fig. 7A). These results suggest that improper AMPK activation during exercise compromises the performance of these mutant mice.

Activation of AMPK and subsequent AMPK-mediated changes in gene expression are crucial steps in the muscle response to exercise. To examine whether β2-deficient muscle has a reduced capacity to upregulate mitochondrial genes, WT and mutant animals (4 to 6 weeks old) were allowed to run on a treadmill set at a constant speed of 15 m/min for 25 min, which was the maximal time β2 mutant mice could run at this speed. Quantitative RT-PCR analysis of gastrocnemius muscle harvested 6 h postexercise revealed that exercise-induced PGC1α and PGC1α target gene expression (e.g., cytochrome *c*, Cox4, and CPT1b) were significantly reduced in β2-deficient muscle (Fig. 7B). Moreover, while AMPK was activated with concomitant phosphorylation of ACC after exercise (2 h) in gastrocnemius muscle of WT animals, no significant exercise-induced increase in pAMPK or pACC levels was observed in β2-deficient muscle (Fig. 7C).

We further investigated the phosphorylation of AMPK substrates in skeletal muscle from β2 mutant animals after exercise (treadmill run). Raptor phosphorylation was increased after exercise in WT muscle but not in β2 mutant muscle (Fig. 7C), although total raptor levels remained unchanged (data not shown). Accordingly, mTOR signaling in β2-deficient muscle was enhanced after exercise, as evidenced by the robust increase in pS6 and p4EBP1 compared to levels in WT muscle (Fig. 7C).

Muscle glycogen is the primary carbohydrate fuel for muscular work during strenuous exercise. To understand why β2 mutant animals have a reduced exercise capacity, we compared basal and postexercise levels of muscle glycogen. The baseline muscle glycogen content of mutant animals was ~38% lower than in WT animals. While glycogen content in the 2-h-postexercise WT muscle was reduced by ~23%, no change in muscle glycogen was observed in the β2 mutant mice following exercise (25 min on the treadmill) (Fig. 7D). We also measured the ATP/AMP ratio immediately after exercise and 2 h postexercise and found that the low ratio present in β2-deficient muscle at baseline was further

decreased after exercise (Fig. 7E and F), indicating the inability to maintain metabolic homeostasis in the absence of normal AMPK activity.

Collectively, our results indicate that the AMPK β2 subunit is important for exercise-induced AMPK activation, AMPK-dependent gene expression, and energy production in addition to its role in muscle glycogenolysis and optimal exercise performance.

DISCUSSION

We dissected the biological roles of the regulatory β2 subunit of AMPK through the analysis of β2-deficient mice. Unlike the widespread expression of the closely related β1 subunit, β2 expression is restricted primarily to brain, heart, kidney, and skeletal muscle, with the last tissue expressing almost exclusively the β2 subunit. Consistent with its unique muscle expression, we found that β2 is required for stress-induced AMPK-regulated functions in skeletal muscle. While we were finishing our studies on the β2 mutant animal, another group reported the generation of another strain of β2-deficient mice and muscle-specific β1/β2-deficient mice (41, 47). While their results are largely consistent with ours, key mechanistic studies in this report determine whether or not the β2 subunit is required for organ-specific baseline phosphorylation of a number of AMPK substrates and whether it is required in skeletal muscle during physiological and pharmacological AMPK activation. Our results also unveil specific roles of β2 subunit in response to nutrient deprivation and exercise-induced stress adaptation.

The β2 mutant mice we generated are overtly normal despite a complete loss of the β2 subunit in all tissues. Adult brain and cardiac muscle express the two β subunits at similar levels, and pAMPK levels were similar in these two tissues in WT and β2 mutant animals. This suggests that the β1 subunit can maintain active AMPK in β2-deficient cardiac muscle and brain at levels similar to those in WT animals. However, the absence of the β2 subunit reduced basal phosphorylation of Raptor, ULK1, and FOXO3 in heart but not in brain. These results suggest that β2-dependent AMPK complex is specifically required to phosphorylate this subset of AMPK substrates in the cardiac muscle but not in the brain. Future studies in various organs will reveal the organ and context-specific function of the two β subunits in regulating AMPK substrate phosphorylation.

In WT skeletal muscle, we found extremely low levels of the β1 subunit, and consequently, only catalytic α subunits associated with the β2 subunit were detected. These results are in contrast to the study by Steinberg et al. (47), in which β1 was found to be predominantly associated with the α catalytic subunit. The relative tissue expression of the two β subunits in wild-type animals was not reported, thus making it difficult to interpret these association results. Despite these discrepancies, the two studies together present a persuasive case for the importance of the β2 subunit in regulating AMPK function in response to stress.

The β2 mutant animals showed essentially normal glucose metabolism, similar to AMPK α1-deficient mice (27), suggesting that the upregulation of the β1 subunit detected in β2-deficient skeletal muscle enables the formation of functional AMPK complexes. In contrast to the basal condition, AICAR-stimulated AMPK phosphorylation and glucose uptake were completely blunted in β2 mutant muscle, suggesting that β2-dependent AMPK function is essential for maximal but not basal glucose import. This phenotype is reminiscent of that in animals lacking the AMPK γ3 subunit (2). Our results, together with these previous studies, indicate that AMPK complexes composed of α2 (27), β2, and γ3 (2) are the predominant source of AMPK activity in muscle. Targeting such complexes with small molecules may provide a relatively specific approach to modulating AMPK activity in skeletal muscle.

The loss of β2 did not cause abnormalities in lipid metabolism, presumably reflecting the normal AMPK function in liver, pancreas, and adipose tissue that is mediated by the predominant β1 subunit in these tissues. A unique finding of our study is the requirement for the β2 subunit in adaptive responses to starvation. In skeletal muscle, AMPK is activated in fasted WT animals with corresponding phosphorylation of ACC but not Raptor and ULK1. While pS6 and p4EBP levels are higher in β2 mutant muscle, fasting induces a dramatic reduction in levels of these phosphorylated proteins, indicating that the remaining AMPKβ1 complexes are sufficient to respond to fasting or that mTOR is also regulated by AMPK-independent mechanisms after fasting. Fasting represents an acute metabolic stress that induces hormonal and cytokine responses to ensure energy homeostasis and maintenance of euglycemia. Thus, hypoglycemia in fasted β2 mutant animals was unexpected because metabolic adaptation to fasting is an important function of the liver, a tissue with very low levels of β2 expression. Glucagon, catecholamines, and ketone bodies also play crucial roles in the metabolic adaptations to fasting; thus, further studies are needed to test whether β2 regulates the production or responses to these molecules or, perhaps, adaptive responses that emanate from the central nervous system.

Skeletal muscle plays a pivotal role in glucose homeostasis. Impaired muscle glucose metabolism induced by the high-fat Western diet is frequently associated with metabolic syndrome. Although the mechanism is not clearly understood and there is some controversy about the extent of its role, AMPK in general opposes the deleterious effects of metabolic syndrome (17, 29, 51, 52). While Fujii et al. (17) observed insulin resistance in FVB animals expressing muscle-specific kinase-dead AMPKα2, Jørgensen et al. (29) did not observe such a phenotype in the C57/BL6 background. Consistent with others (41, 47), our study shows that AMPK complexes in muscle contain primarily the β2 subunit, and β2 mutant animals maintained on an HFD have high body fat (compared to wild-type animals on an HFD) and manifest features of metabolic syndrome.

Muscle AMPK signaling has been shown to be impaired by obesity (35). Consistent with this result, we found that muscles of wild-type mice fed an HFD had reduced pAMPK levels. pAMPK levels were further reduced in β2 mutant animals, suggesting that β2 is an important regulator of muscle AMPK activity during metabolic stress induced by an HFD. Despite reduced pAMPK and pRaptor levels in skeletal muscle from animals maintained on an HFD, S6 and 4EBP1 phosphorylation was significantly reduced in both WT and β2 mutant skeletal muscle, indicating AMPK-independent mTOR regulation in this tissue in response to an HFD. Unlike muscle from WT animals on HFD, Raptor phosphorylation in β2-deficient muscle from animals on an HFD was not reduced compared to that in muscles from animals on normal chow. This again points to a complex regulation of the AMPK mTOR axis in mice exposed to a Western diet.

One manner in which glucose metabolism is increased by AMPK is through increasing translocation of glucose transporters to the cell surface (36, 39, 43, 55). Consistent with the study of Steinberg et al. (47), total Glut4 levels were equivalent in muscle

from β2 mutant mice and wild-type mice maintained on a normal diet. However, in β2 mutant animals on an HFD, we found that surface Glut4 levels decreased significantly, suggesting that Glut4 translocation is regulated by AMPK complexes containing β2. Another mechanism by which an HFD alters glucose metabolism is via inhibition of glucose phosphorylation (18); however, a role for β2 in regulating this process has not been investigated.

Increases in aerobic metabolism, insulin resistance, and obesity are all induced by an HFD and are risk factors for the development of metabolic syndrome in humans (8). The loss of AMPK activity in skeletal muscles of β2-deficient mice also leads to abnormalities reminiscent of metabolic syndrome. In accord with these findings, AMPK activating agents can reverse metabolic syndrome in genetically obese rodents and are also effective in treating diabetic patients with reduced insulin sensitivity (16, 23). Results obtained in studies of β2 mutant mice strongly support a role for this AMPK subunit in abnormalities associated with metabolic syndrome and suggest that drugs that activate AMPK complexes containing the β2 subunit could be used to treat diabetes and obesity.

During fasting, skeletal muscle glycogen is broken down to glucose to provide a valuable source of energy (2, 6, 12, 32). AMPK activation in skeletal muscle during fasting also promotes energy conservation through the inhibition of biosynthetic processes (11). The failure of β2 mutant animals to maintain energy balance during fasting indicates the role of this AMPK subunit in this adaptive response, which includes hepatic gluconeogenesis, fatty acid oxidation, and glycogen breakdown in liver and skeletal muscle. The reduced glycogen levels we and others (47) observed in skeletal muscles of β2-deficient animals have also been reported for AMPK α2 and γ3 mutant animals (2, 51). Multiple mechanisms regulate glycogen synthesis and breakdown that could account for this deficiency (4). For example, glycogen synthesis is regulated by insulin-mediated Akt activation through its inhibition of GSK3β (34), a pathway that may also be influenced by AMPK. Alternatively, β2-dependent AMPK activity might be required for muscle glycogen accumulation through the allosteric activation of glycogen synthase caused by increased glucose-6-phosphate (24). In addition to the low basal glycogen levels, our results suggest a crucial role for β2-dependent AMPK activity in fasting-induced glycogenolysis. It is worth noting in this regard that both AICAR and AMP enhance glycogen phosphorylase activity and glycogenolysis in rat skeletal muscle (56).

An important finding of our study is that mice lacking β2, which constitutes >90% of the total β subunit in skeletal muscle, demonstrated poor exercise performance. The skeletal muscle in these mutant mice also has lower basal energy content, as basal glycogen levels are reduced. In addition, while WT muscle showed 23% reduced glycogen content after 2 h of exercise, glycogen levels did not change in β2 mutant animals. This is likely due to failure of glycogen breakdown in response to exercise, suggesting that AMPK complexes containing β2 enhance glycogen phosphorylase activity (56). Alternatively, reduced AMPK activity could increase glycogen synthase (GS) activity specifically in the postexercise muscle (thus increasing postexercise glycogen resynthesis). This is consistent with studies showing that AMPKβ2 inhibits glycogen synthase in renal tubules (5) and muscle (15).

In contrast to nutrient stress (fasting and HFD), we found a direct negative relationship between AMPK and mTOR signaling during exercise. AMPK was activated in muscle in animals that were exercised, and this kept mTOR signaling at low levels (no significant increase in pS6 and p4EBP1) in WT muscle. In sharp contrast, levels of phosphorylated S6 and 4EBP1 increased in muscle from β2-deficient animals after exercise, suggesting that AMPKβ2 complexes are essential for reducing mTOR signaling during exercise. Importantly, we also found that β2 is necessary for exercise-induced AMPK activity and for increased transcription of PGC1α and PGC1α target genes. In contrast, α2-deficient skeletal muscle shows decreased PGC1α basal transcriptional activity but normal exercise-induced activity, suggesting that compensation from the remaining α1 subunit promotes exercise-induced AMPK activation (28). In the study by Steinberg et al. (47), there was a trend toward reduced expression of PGC1α and Cpt1b in β2-deficient muscle after exercise. Our study shows that expression of PGC1α and other mitochondrial genes is significantly reduced in gastrocnemius muscle 6 h postexercise. While the muscle source and time of collection were not reported in their study (47), it should be noted that gene expression can vary significantly with time and muscle type after physical exercise. This could account for some of the discrepancies observed between these studies.

Although it is clear that exercise induces activation and nuclear translocation of AMPK (38, 40), and decreased AMPK activity reduces voluntary exercise (51), questions remain with regard to the role of AMPK during muscle contraction (27, 28). AMPK activation in skeletal muscle during exercise improves athletic performance (28), and mice treated with AMPK activating compounds exhibit superendurance (26, 40). The current results provide compelling evidence that AMPK complexes containing β2 are crucial for muscle contraction during exercise performance, and they provide an opportunity to explore the therapeutic value of agents that target β2-containing AMPK complexes to promote AMPK activity specifically in muscle.

ACKNOWLEDGMENTS

We thank John Holloszy and Dong Ho Han for their help with the muscle glucose uptake studies, Anne Brunet for sharing the FOXO3 antibodies, Amy Strickland for conducting the treadmill tests and rotarod tests, Robert Baloh for conducting the nerve conduction velocity tests, and Richard (Scott) Dunn for the MRI studies.

This work was supported by National Institutes of Health (NIH) Neuroscience Blueprint Core Grant NS057105 (to Washington University), NIH grant P30 DK56341 to the CNRU, the HOPE Center for Neurological Disorders, and NIH grants AG13730 and NS040745 (to J.M.) and by the Division of Hematology and Oncology, Cincinnati Children's Hospital Medical Center (to B.D.).

REFERENCES

1. **Baena-González E, Rolland F, Thevelein JM, Sheen J.** 2007. A central integrator of transcription networks in plant stress and energy signaling. Nature **448**:938–942.
2. **Barnes BR, et al.** 2004. The 5′-AMP-activated protein kinase gamma3 isoform has a key role in carbohydrate and lipid metabolism in glycolytic skeletal muscle. J. Biol. Chem. **279**:38441–38447.
3. **Barnes BR, et al.** 2005. 5-AMP-activated protein kinase regulates skeletal muscle glycogen content and ergogenics. FASEB J. **19**:773–779.
4. **Bouskila M, et al.** 2010. Allosteric regulation of glycogen synthase controls glycogen synthesis in muscle. Cell Metab. **12**:456–466.
5. **Cammisotto PG, Londono I, Gingras D, Bendayan M.** 2008. Control of glycogen synthase through ADIPOR1-AMPK pathway in renal distal tubules of normal and diabetic rats. Am. J. Physiol. Renal Physiol. **294**:F881–F889.
6. **Cantó C, et al.** 2010. Interdependence of AMPK and SIRT1 for metabolic adaptation to fasting and exercise in skeletal muscle. Cell Metab. **11**:213–219.
7. **Chen Z, et al.** 1999. Expression of the AMP-activated protein kinase beta1 and beta2 subunits in skeletal muscle. FEBS Lett. **460**:343–348.

8. **Cornier M, et al.** 2008. The metabolic syndrome. Endocr. Rev. **29**:777–822.
9. **Crute BE, Seefeld K, Gamble J, Kemp BE, Witters LA.** 1998. Functional domains of the alpha1 catalytic subunit of the AMP-activated protein kinase. J. Biol. Chem. **273**:35347–35354.
10. **Dasgupta B, Milbrandt J.** 2009. AMP-activated protein kinase phosphorylates retinoblastoma protein to control mammalian brain development. Dev. Cell **16**:256–270.
11. **Dasgupta B, Milbrandt J.** 2007. Resveratrol stimulates AMP kinase activity in neurons. Proc. Natl. Acad. Sci. U. S. A. **104**:7217–7222.
12. **de Lange P, et al.** 2006. Sequential changes in the signal transduction responses of skeletal muscle following food deprivation. FASEB J. **20**: 2579–2581. (Erratum, **21**:629, 2007.)
13. **Derave W, et al.** 2000. Dissociation of AMP-activated protein kinase activation and glucose transport in contracting slow-twitch muscle. Diabetes **49**:1281–1287.
14. **Egan DF, et al.** 2011. Phosphorylation of ULK1 (hATG1) by AMP-activated protein kinase connects energy sensing to mitophagy. Science **331**:456–461.
15. **Fediuc S, Gaidhu MP, Ceddia RB.** 2006. Inhibition of insulin-stimulated glycogen synthesis by 5-aminoimidasole-4-carboxamide-1-beta-D-ribofuranoside-induced adenosine 5′-monophosphate-activated protein kinase activation: interactions with Akt, glycogen synthase kinase 3-3alpha/beta, and glycogen synthase in isolated rat soleus muscle. Endocrinology **147**:5170–5177.
16. **Fryer LG, Parbu-Patel A, Carling D.** 2002. The anti-diabetic drugs rosiglitazone and metformin stimulate AMP-activated protein kinase through distinct signaling pathways. J. Biol. Chem. **277**:25226–25232.
17. **Fujii N, et al.** 2008. Ablation of AMP-activated protein kinase alpha2 activity exacerbates insulin resistance induced by high-fat feeding of mice. Diabetes **57**:2958–2966.
18. **Furler SM, Oakes ND, Watkinson AL, Kraegen EW.** 1997. A high-fat diet influences insulin-stimulated posttransport muscle glucose metabolism in rats. Metabolism **46**:1101–1106.
19. **Greer EL, et al.** 2007. An AMPK-FOXO pathway mediates longevity induced by a novel method of dietary restriction in C. elegans. Curr. Biol. **17**:1646–1656.
20. **Greer EL, et al.** 2007. The energy sensor AMP-activated protein kinase directly regulates the mammalian FOXO3 transcription factor. J. Biol. Chem. **282**:30107–30119.
21. **Gwinn DM, et al.** 2008. AMPK phosphorylation of raptor mediates a metabolic checkpoint. Mol. Cell **30**:214–226.
22. **Hansen PA, Gulve EA, Holloszy JO.** 1994. Suitability of 2-deoxyglucose for in vitro measurement of glucose transport activity in skeletal muscle. J. Appl. Physiol. **76**:979–985.
23. **Hardie DG.** 2004. AMP-activated protein kinase: a master switch in glucose and lipid metabolism. Rev. Endocr. Metab. Disord. **5**:119–125.
24. **Hunter RW, Treebak JT, Wojtaszewski JF, Sakamoto K.** 2011. Molecular mechanism by which AMP-activated protein kinase activation promotes glycogen accumulation in muscle. Diabetes **60**:766–774.
25. **Inoki K, Zhu T, Guan KL.** 2003. TSC2 mediates cellular energy response to control cell growth and survival. Cell **115**:577–590.
26. **Jäger S, Handschin C, St-Pierre J, Spiegelman BM.** 2007. AMP-activated protein kinase (AMPK) action in skeletal muscle via direct phosphorylation of PGC-1alpha. Proc. Natl. Acad. Sci. U. S. A. **104**:12017–12022.
27. **Jørgensen SB, et al.** 2004. Knockout of the alpha2 but not alpha1 5′-AMP-activated protein kinase isoform abolishes 5-aminoimidazole-4-carboxamide-1-beta-4-ribofuranoside but not contraction-induced glucose uptake in skeletal muscle. J. Biol. Chem. **279**:1070–1079.
28. **Jørgensen SB, et al.** 2005. Effects of alpha-AMPK knockout on exercise-induced gene activation in mouse skeletal muscle. FASEB J. **19**:1146–1148.
29. **Jørgensen SB, O'Neill HM, Hewitt K, Kemp BE, Steinberg GR.** 2009. Reduced AMP-activated protein kinase activity in mouse skeletal muscle does not exacerbate the development of insulin resistance with obesity. Diabetologia **52**:2395–2404.
30. **Kim JY, et al.** 2000. High-fat diet-induced muscle insulin resistance: relationship to visceral fat mass. Am. J. Physiol. Regul. Integr. Comp. Physiol. **279**:R2057–R2065.
31. **Kim J, Kundu M, Viollet B, Guan KL.** 2011. AMPK and mTOR regulate autophagy through direct phosphorylation of Ulk1. Nat. Cell Biol. **13**: 132–141.
32. **Kokubun E, Hirabara SM, Fiamoncini J, Curi R, Haebisch H.** 2009. Changes of glycogen content in liver, skeletal muscle, and heart from fasted rats. Cell Biochem. Funct. **27**:488–495.
33. **Lee JH, et al.** 2007. Energy-dependent regulation of cell structure by AMP-activated protein kinase. Nature **447**:1017–1020.
34. **Lee J, Kim MS.** 2007. The role of GSK3 in glucose homeostasis and the development of insulin resistance. Diabetes Res. Clin. Pract. **77S**:S49–S57.
35. **Lee-Young RS, et al.** 2011. Obesity impairs skeletal muscle AMPK signaling during exercise: role of AMPKα2 in the regulation of exercise capacity in vivo. Int. J. Obes. (Lond.) **35**:982–989.
36. **Li J, et al.** 2004. Role of the nitric oxide pathway in AMPK-mediated glucose uptake and GLUT4 translocation in heart muscle. Am. J. Physiol. Endocrinol. Metab. **287**:E834–E841.
37. **McBride A, Ghilagaber S, Nikolaev A, Hardie DG.** 2009. The glycogen-binding domain on the AMPK beta subunit allows the kinase to act as a glycogen sensor. Cell Metab. **9**:23–34.
38. **McGee SL, et al.** 2003. Exercise increases nuclear AMPK alpha2 in human skeletal muscle. Diabetes **52**:926–928.
39. **Mu J, Jr, Brozinick JT, Valladares O, Bucan M, Birnbaum MJ.** 2001. A role for AMP-activated protein kinase in contraction- and hypoxia-regulated glucose transport in skeletal muscle. Mol. Cell **7**:1085–1094.
40. **Narkar VA, et al.** 2008. AMPK and PPARdelta agonists are exercise mimetics. Cell **134**:405–415.
41. **O'Neill HM, et al.** 2011. AMP-activated protein kinase (AMPK) beta1beta2 muscle null mice reveal an essential role for AMPK in maintaining mitochondrial content and glucose uptake during exercise. Proc. Natl. Acad. Sci. U. S. A. **108**:16092–16097.
42. **Polekhina G, et al.** 2003. AMPK beta subunit targets metabolic stress sensing to glycogen. Curr. Biol. **13**:867–871.
43. **Sarabia V, Lam L, Burdett E, Leiter LA, Klip A.** 1992. Glucose transport in human skeletal muscle cells in culture. Stimulation by insulin and metformin. J. Clin. Invest. **90**:1386–1395.
44. **Schapira G, Dobocz I, Piau JP, Delain E.** 1974. An improved technique for preparation of skeletal muscle cell plasma membrane. Biochim. Biophys. Acta Biomembranes **345**:348–358.
45. **Schmidt MC, McCartney RR.** 2000. Beta-subunits of Snf1 kinase are required for kinase function and substrate definition. EMBO J. **19**:4936–4943.
46. **Spasić MR, Callaerts P, Norga KK.** 2008. Drosophila alicorn is a neuronal maintenance factor protecting against activity-induced retinal degeneration. J. Neurosci. **28**:6419–6429.
47. **Steinberg GR, et al.** 2010. Whole body deletion of AMP-activated protein kinase β2 reduces muscle AMPK activity and exercise capacity. J. Biol. Chem. **285**:37198–37209.
48. **Thornton C, Snowden MA, Carling D.** 1998. Identification of a novel AMP-activated protein kinase beta subunit isoform that is highly expressed in skeletal muscle. J. Biol. Chem. **273**:12443–12450.
49. **Treebak JT, et al.** 2010. Identification of a novel phosphorylation site on TBC1D4 regulated by AMP-activated protein kinase in skeletal muscle. Am. J. Physiol. Cell Physiol. **298**:C377–C385.
50. **Turnley AM, et al.** 1999. Cellular distribution and developmental expression of AMP-activated protein kinase isoforms in mouse central nervous system. J. Neurochem. **72**:1707–1716.
51. **Villena JA, et al.** 2004. Induced adiposity and adipocyte hypertrophy in mice lacking the AMP-activated protein kinase-alpha2 subunit. Diabetes **53**:2242–2249.
52. **Viollet B, et al.** 2003. The AMP-activated protein kinase alpha2 catalytic subunit controls whole-body insulin sensitivity. J. Clin. Invest. **111**:91–98.
53. **Winder WW, Hardie DG.** 1996. Inactivation of acetyl-CoA carboxylase and activation of AMP-activated protein kinase in muscle during exercise. Am. J. Physiol. **270**:299–304.
54. **Xue B, Kahn BB.** 2006. AMPK integrates nutrient and hormonal signals to regulate food intake and energy balance through effects in the hypothalamus and peripheral tissues. J. Physiol. **574**:73–83.
55. **Yang J, Holman GD.** 2006. Long-term metformin treatment stimulates cardiomyocyte glucose transport through an AMP-activated protein kinase-dependent reduction in GLUT4 endocytosis. Endocrinology **147**: 2728–2736.
56. **Young ME, Radda GK, Leighton B.** 1996. Activation of glycogen phosphorylase and glycogenolysis in rat skeletal muscle by AICAR—an activator of AMP-activated protein kinase. FEBS Lett. **382**:43–47.